INVESTIGATION OF STABILITY OF CORONA ION SOURCE AND ELECTRIC FIELD IN ION MOBILITY SPECTROMETRY

Arian Fateh Borkhari, Ladislav Moravský, Štefan Matejčík

Department of Experimental Physics, Comenius University
Mlynská dolina F2, 842 48 Bratislava, Slovakia

E-mail: borkhari1@uniba.sk

The stability of the operation of the negative corona discharge ion source for the Ion Mobility Spectrometry (IMS) has been studied. The temporal stability of the ion current was investigated as a function of wire diameter (20, 50, and 100μm) and wire material (the high-voltage electrode). The ion current generation efficiency was increasing for thin microwires. The temporal ion current stability was improving with the increasing electrode gap between the high voltage electrode and the hollow electrode (from 1 up to 10mm) and with decreasing of the wire diameter. The impact of the electrode material was low on the stability of the ion current. Additionally, we have simulated the configuration of the electric fields in the ion source and the IMS drift-tube.

1. Introduction

Ion Mobility Spectrometry (IMS) is an analytical technique for the separation of ions in the gaseous phase based on the differences in the mobilities of the ions under an electric field. The ion source is one of the main parts of IMS, besides the reaction chamber, shutter gride, drift tube, and detector [1-7]. The ion source serves as a source of reactant ions (RI) of positive or negative polarity, which are used for ionization of the sample in the reaction region and formation of gas-phase ions. Several different ion sources for IMS systems have been developed, such as radioactive ion sources, discharge ion sources, thermal ionisation, photoionization, X-ray ionization, electrospray ionization, atmospheric pressure electron gun, etc. [5-7].

In the present work, we present a study of the stability of the corona discharge ion source in negative polarity. The selection of a suitable material and geometry (radius of wire and the electrode gap) of the corona discharge electrode (microwire) result in the improvement of the stability of the ion current, the improvement of the ion intensity, and thus the sensitivity of IMS [8-11].

2. Experimental Setup

Figure 1 shows the experimental setup to study the operation of the corona discharge as an ion source for IMS. In this study, we have used a wire-to-plane configuration with the hollow in the plane electrode to negative corona discharge. The hollow electrode can be spatially adjusted in three directions, and the electrode separation can be controlled to 1 micrometre. A microwire was used as the high voltage electrode with different diameters (20, 50, and 100μm) and materials (tungsten, copper, platinum, cobalt, stainless steel), while the plane electrode material was brass. An additional electrode, Faraday plate was placed behind the plane electrode. Between the plane electrode and the Faraday plate, an extraction voltage (V_{HE}) was applied. The Faraday plate was equipped with a protection circuit consisting of back-to-back diodes. The electric current was amplified with a transimpedance current to voltage amplifier and measured using an oscilloscope (Tektronix TDS2022B). The high voltage part of the electrical circuit consisted of a high voltage power supply (Fug HCP 35-20000), with a resistor (15MΩ) to limit the DC current (10μA). The second DC power supply (Heinzinger LNG 350-03) supports the high voltage up to 350V to the plan electrode (HE).

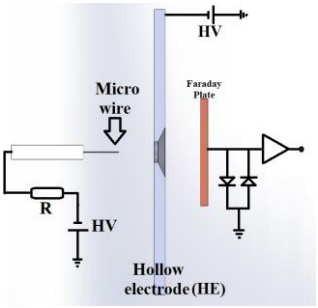

Fig. 1. The schematic view of the experimental setup for ion generation.

3. Results

Figure 2 shows the measured dependence of the negative corona current on the applied negative high voltage for different wire diameters (20, 50, and 100µm) and various electrode gap distances (from 3 up to 10mm). The high-voltage electrode was made of tungsten. The ion current was measured for different voltages of the hollow electrode (V_{HE} = 0, 50, 100, 200, and 350V). The potential V_{HE} pushes the ions generated by corona discharge to the detector (Faraday plate). We have observed that the measured current on the Faraday plate increases with the increasing HV potential on the wire electrode (due to increase of charge current) and also with the increasing HE potential, due to improvement of the ion transport to the Faraday plate.

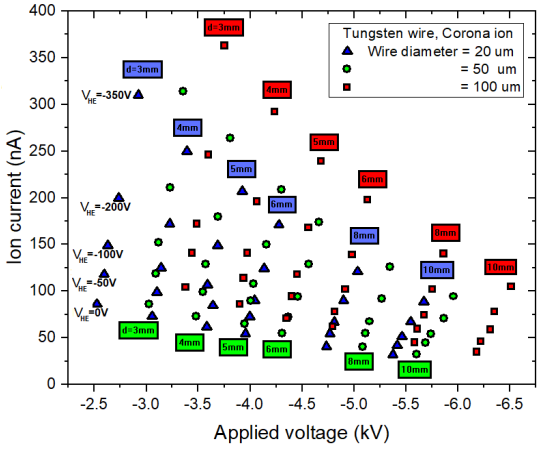

Fig. 2. Current-voltage characteristics for different diameters of the tungsten wire.

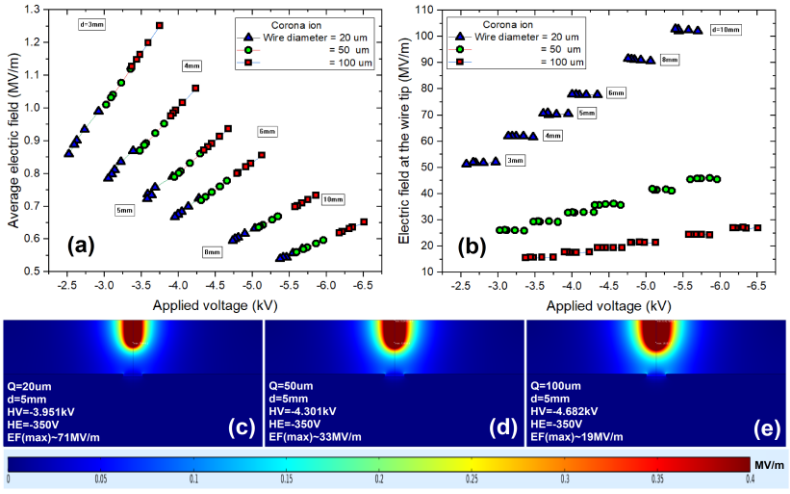

Fig. 3. Electric field strength for different diameters of the wire.

The diameter of the microwire affects the ion generation and its stability (Fig. 3) due to changes in the electric field. The average electric field between the electrodes is illustrated in Fig. 3 a) for 20, 50, and 100µm wire diameters. The experimental voltage values were used to simulate the local electric field strength at the microwire tip (Fig. 3 b). Based on Fig. 3 a), the average electric field increases with the decreasing of gap distance, whereas increased gap causes the increase of the local maximum electric

field at the wire tip (Fig. 3 b). The graphical simulation in Fig. 3 c, d, and e) is presented to validate the plotted results in Fig. 3 a) and Fig. 3 b).

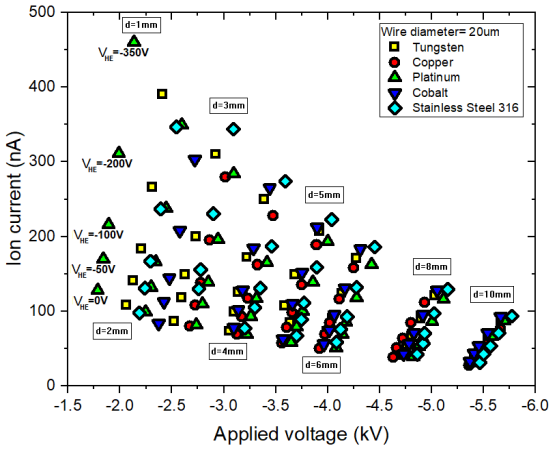

Fig. 4. Experimental data: current-voltage characteristics for different wire materials.

The effect of the material of the wire electrode on the current-voltage characteristics is presented in Fig. 4. The measured current-voltage characteristics were performed for different wire materials (tungsten, copper, platinum, cobalt, and stainless-steel), different discharge gaps and V_{HE} potentials. The diameter of all wires was 20µm. Figure 5 shows the values of the electric field strength for different wire materials and different discharge currents. The average electric field is presented in Fig. 5 a). The local electric field strength at the wire tip was calculated for the applied voltages and different wire materials (Fig. 5 b). The field strengths are illustrated in Fig 5 c, d, and e where the microwire has 20µm diameter for 1, 5, and 10mm gap distance.

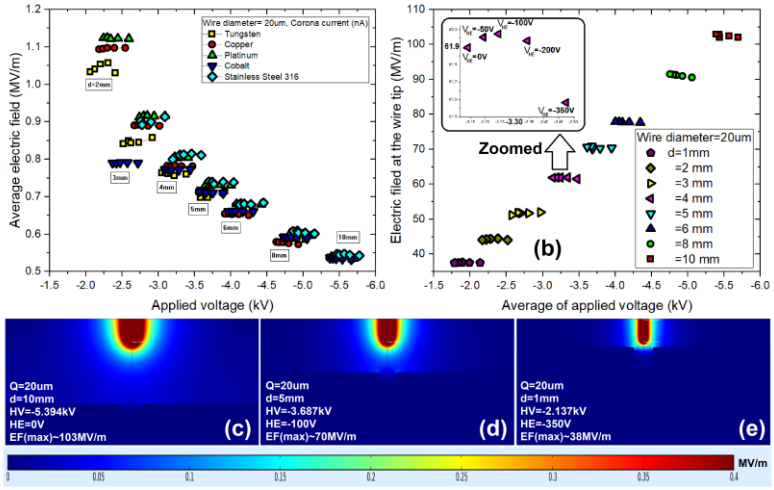

Fig. 5. The strength of the local electric field for different wire discharge gaps.

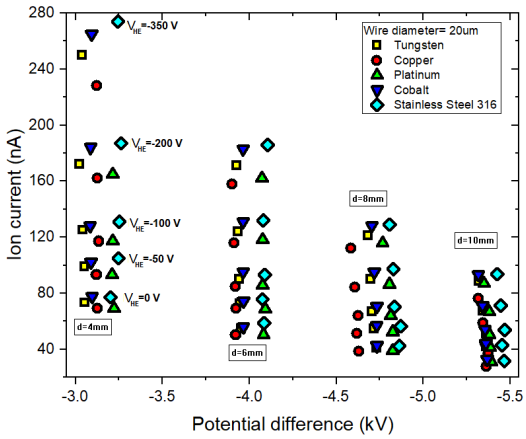

Fig. 6. Experimental I vs V plots for different wire materials.

Figure 6 shows the dependence of the ion current on the potential differences between the electrodes. The high value of relative standard deviation was observed for thick wire (100μm). These results are shown in Fig. 7.

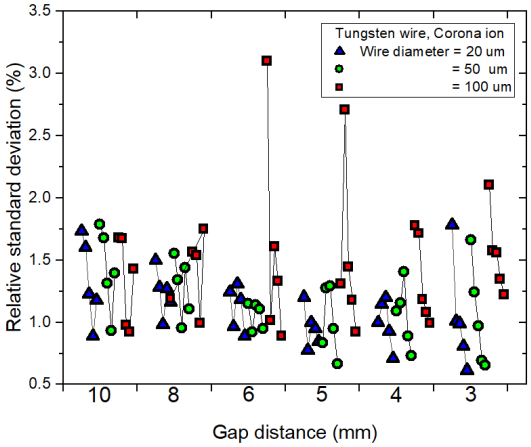

Fig. 7. Relative standard deviation (%) of the temporal stability of ion current for different diameters of the tungsten wire.

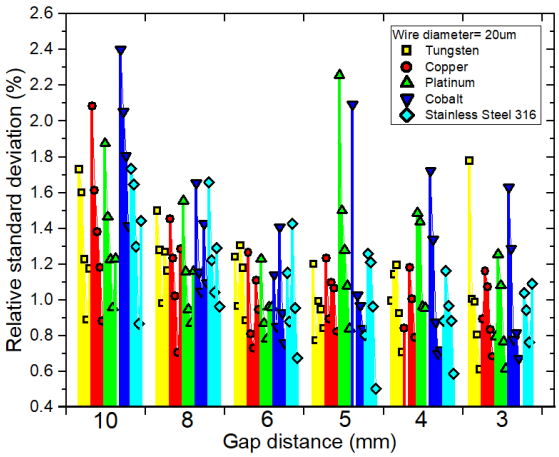

Fig. 8. Relative standard deviation (%) of signal stability of Corona ions for different wire materials.

The relative standard deviation has been calculated for ion currents (Fig. 8), which have been related to different wire materials. We found the proper gap-distance for the generation of a more stable ion signal based on the geometrical configuration of electrodes. Fig. 8 shows the more stable signals at d=5 and 6mm for most of the materials.

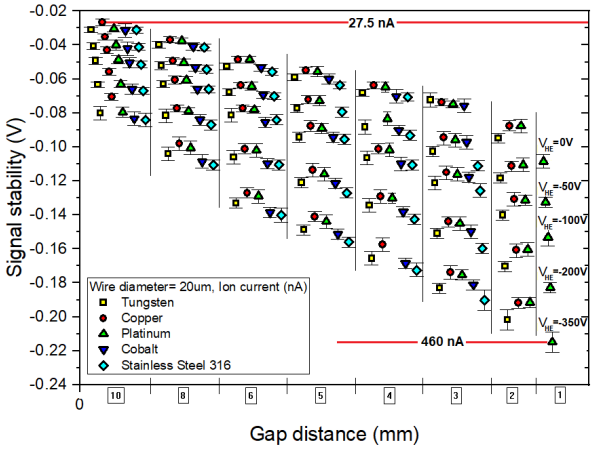

Fig. 9. Experimental data of signal stability of Corona ions for different wire materials.

The statistical analysis of the temporal stability of the ion current is presented in Fig. 9 for different wire materials and different electrode gaps. The result shows that the stability of the discharge current

was not substantially affected by the wire material. However, we see a week effect of the electrode gap for smaller gaps, the relative temporal stability of the discharge current was higher. We relate it to the strength of the electric field. In addition to the simulation of the electric fields in the ion source, we have performed simulations of the electric fields in the IMS (Fig. 10). For the functionality of the IMS, the strength of the electric field along the axis of the IMS drift tube is of great importance (Fig. 11). Figure 11 shows that the homogeneity of the electric field in the drift tube is quite good and that the inhomogeneities appear only in the ions source, shutter gride, and at the detector. However, in the future, we should further improve the homogeneity of the electric field in the IMS.

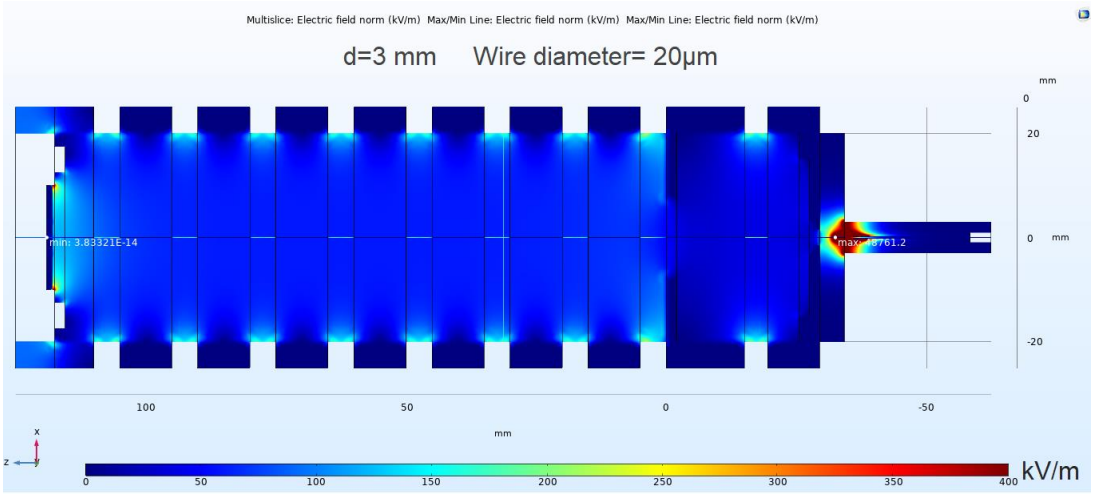

Fig. 10. Simulation of a homogeneous electric field in the IMS drift-tube.

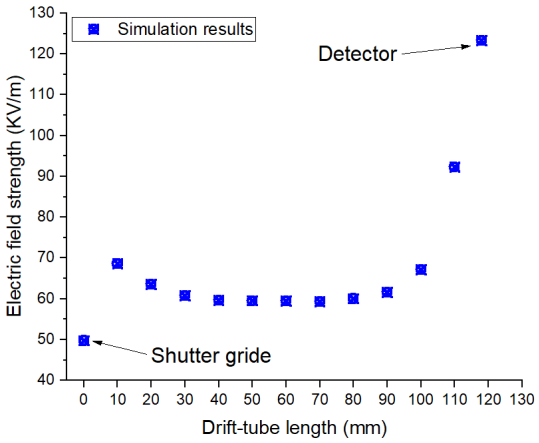

Fig. 11. Electric field strength at the axis of IMS drift-tube.

4. Conclusion

We have presented an experimental study concerning the temporal stability of the generation of the ion current by the Corona Ion Source in IMS. Different materials and diameters have been investigated for the high voltage electrode (microwire). Experimental data including the current-voltage characteristics, the average electric field between the electrodes, and the local electric fields at the tip of the wire electrode were determined. The experimental studies and simulations were carried out for the microwires (20, 50, and 100µm) diameter and different wire materials (tungsten, copper, platinum, cobalt, and stainless steel). The improved temporal stability of the ion current was observed for the smaller wire diameter (20µm). The impact of the electrode material on the temporal stability of the ion current was low. Based on the practical values of electrical parameters of the IMS, we have simulated a 2D map of the electric field in IMS and the axial dependence of the strength of the electric field.

5. References

[1] Stano M, Safonov E, Kucera M, Matejcik Š 2008 Chem. Listy 102 s1414−s1417.
[2] Sabo M, et al. 2015 Analytical Chemistry 7 14 7389–7394.
[3] Sabo M, et al. 2010 International Journal of Mass Spectrometry 293 23–27.
[4] Gravendeel B 1987 ebook: doi:10.6100/IR256688.
[5] Raizer Y P 1987 Springer Berlin.
[6] Scheffler P, Gessner C, Gericke K H 2000 Braunschweig (D).
[7] Gunzer F, Ulrich A, Baether W 2010 Int. J. Ion Mobil. Spec. 13:9–16.
[8] Kim H J, Han B, Woo C G and Kim Y J 2016 IEEE Transactions on Industry Applications pp 99.
[9] Yehia A and Mizuno A 2008 Int. J. of Plasma Environmental Sc. & Tec. Vol.2 No.1 pp 44-49.
[10] Petrov A A 2009 IEEE Transactions on plasma science Vol. 37, No. 7.
[11] Horvath G, Skalny J D, Orszagh J, Vladoiu R, Mason N J 2010 Plasma Chem Plasma Process 30:43–53.